

*Work supported in part by the National Science Foundation.

†Present Address: Nuclear Assurance Corporation, 24 Executive Park West, Atlanta, Ga. 30329.

¹L. Van Hove, Phys. Rev. 95, 1374 (1954); W. Marshall and R. D. Lowde, Rept. Progr. Phys. 31-II, 705 (1968).

²C. G. Windsor, in *Neutron Inelastic Scattering* (International Atomic Energy Agency, Vienna, 1968), Vol. II, p. 83; Proc. Roy. Soc. (London) 91, 353 (1967).

³R. E. Watson, M. Blume, and G. H. Vineyard, Phys. Rev. 181, 811 (1969).

⁴R. E. Watson, M. Blume, and G. H. Vineyard, Phys.

Rev. B 2, 684 (1970).

⁵J. D. Patterson and G. L. Jones, Phys. Rev. B 3, 131 (1971).

⁶M. Blume, R. E. Watson, and G. H. Vineyard, Bull. Am. Phys. Soc. 16, 629 (1971).

⁷M. E. Fisher, Am. J. Phys. 32, 343 (1964).

⁸Y. I. Chang, G. C. Summerfield, and D. M. Kaplan, Phys. Rev. B 3, 3052 (1971).

⁹D. M. Kaplan and G. C. Summerfield, Phys. Rev. 187, 639 (1969).

¹⁰D. M. Kaplan, Transport Theory Statist. Phys. 1, 81 (1971).

de Haas-van Alphen Effect in Antiferromagnetic Cr-Rich Alloys*

E. J. Gutman[†] and J. L. Stanford

*Institute for Atomic Research and Department of Physics, Iowa State University,
Ames, Iowa 50010*

(Received 11 June 1971)

de Haas-van Alphen measurements have been made on Cr-rich alloys with up to 2-at. % V and 1-at. % Mn. In the crystals in which the antiferromagnetic wave vector \vec{q} is incommensurate with a reciprocal-lattice vector, the changes in three of the frequencies associated with hole ellipsoids at N are consistent with changes in \vec{q} , rather than with a geometrical change in the size of the hole ellipsoids upon alloying. In the crystal in which \vec{q} is commensurate with a reciprocal-lattice vector, several frequency branches were observed. The angular dependence of these branches is consistent with simple ellipsoid models of the Fermi surface.

I. INTRODUCTION

In recent years the antiferromagnetism of Cr has been extensively studied and the experimental results are in agreement with an itinerant electron model of antiferromagnetism. In this model the electron gas acts collectively to produce a spatially varying spin density with wave vector \vec{q} which in general is not commensurate with a reciprocal-lattice vector.

The effects on the physical properties of Cr due to alloying V, Mn, and other metals with Cr have also been studied. The effect on the Néel temperature T_N , for example, due to alloying V, Mn, and Mo with Cr is shown in Fig. 1. It is seen that V decreases the Néel temperature while Mn increases T_N .¹⁻¹¹ These two metals have a similar effect on the magnitude of \vec{q} .⁸ The changes in T_N and \vec{q} have been interpreted as arising from a modification of the Fermi surface (FS) of Cr due to alloying.¹ Since, as shown in Fig. 1, as little as 4-at. % V in Cr lowers T_N below 4 K, one may be able to observe the modified FS of Cr in the paramagnetic state.

Lomer^{12,13} first proposed a model of the FS of Cr and suggested that the antiferromagnetic state was stabilized by flat portions of the FS. Loucks¹⁴ calculated the FS of Cr using an augmented-plane-

wave method, and his result for the (100) plane is shown in Fig. 2. Loucks did not find hole ellipsoids at N (shown by dashes in Fig. 2), although experimental evidence¹⁵ indicates they are present. The flat portions of the hole octahedron and body of the electron jack are separated by $q = (2\pi/a)(1 - \delta)$, $\delta \sim 0.05$.

One method used to determine the FS of a metal is the de Haas-van Alphen (dHvA) effect. dHvA measurements have been made on pure Cr in a single- \vec{q} state.¹⁵ Experiments have shown that usually there are three spin-density wave vectors present in a Cr crystal. However, if the crystal is cooled through T_N in the presence of a large magnetic field (field cooling) the crystal will contain only one \vec{q} .¹⁶ The resulting dHvA spectrum obtained from a crystal with single \vec{q} is quite complex, and not all of the observed branches in the spectrum have been interpreted. dHvA measurements in Cr-alloy crystals¹⁷ will provide more insight into the FS and antiferromagnetic state of Cr. In the present paper, we report the first detailed FS measurements on a series of antiferromagnetic Cr-V and Cr-Mn alloys.

II. EXPERIMENT

The dHvA samples were prepared from single- or

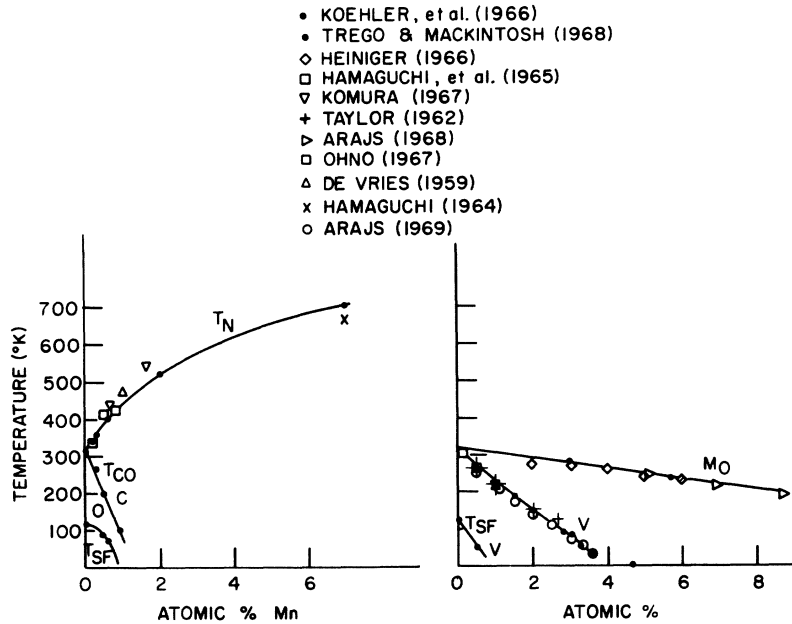


FIG. 1. Change in Néel temperature T_N due to alloying V, Mn, and Mo with Cr. T_{SF} is the spin-flip temperature. T_{CO} is the temperature at which \vec{q} changes from being incommensurate with the chemical lattice (or oscillatory) to being commensurate with the chemical lattice.

bicrystal ingots grown in the Ames Laboratory. The impurity concentrations were determined by chemical analysis and found to be 2.0-at. % V, 1.02-at. % V, 0.58-at. % V, 0.2-at. % V, 0.09-at. % V, 0.03-at. % Mn, 0.04-at. % Mn, 0.16-at. % Mn, 0.45-at. % Mn, and 0.91-at. % Mn. The residual resistance ratio (RRR) of the Cr starting material was approximately 300 while in the 2.0-at. % V sample the RRR was approximately 11. All of the dHvA samples were determined to be single crystals by back-reflection Laue photographs.

The dHvA signal was observed by using a field-

modulation technique.¹⁸ The apparatus has been previously described by Stone¹⁹ and Boyle.²⁰ The amplitude of the dHvA signals at high fields varied from 2000 μV p - p in pure Cr to about 10 μV p - p in the 2.0-at. % V sample. The small-amplitude modulating field produces harmonics of the oscillatory magnetization of the Cr samples. The amplitude of the n th harmonic of the magnetization is proportional to a Bessel function of order n . The argument of the Bessel function is $2\pi(\delta H/f)$, where δH is the amplitude of the modulating field and f is a dHvA frequency. Hence, by varying the amplitude of the

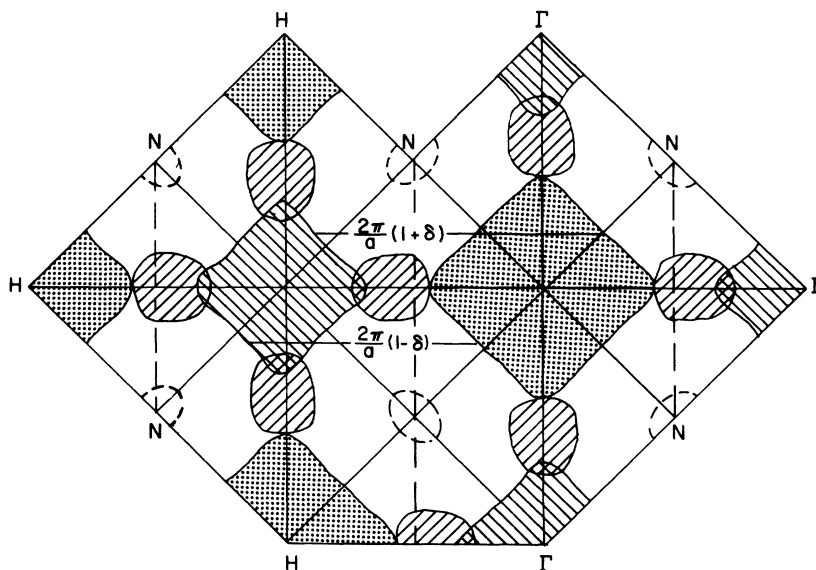


FIG. 2. Louck's calculation for the FS of Cr in a (100) plane. Experimental evidence indicates the presence of hole pockets at N although they are not present in Louck's calculations. The spin-density wave vectors $\vec{q} = (2\pi/a)(1 - \delta)[001]$ and $\vec{q}^* = (2\pi/a)(1 + \delta)[001]$ are also shown.

modulating field, one can either enhance or cancel out a particular dHvA frequency. The argument was adjusted to give maximum amplitude for the second harmonic signal of the $(4-6) \times 10^6$ -G dHvA frequency in the incommensurate samples. In the commensurate crystals, the amplitude of the modulating field was adjusted for maximum amplitudes of the $(10$ and $20) \times 10^6$ -G dHvA signals. The magnetic field was obtained from a compensated Varian superconducting solenoid with a maximum field of 62 kG and inhomogeneities on the order of 10^{-5} in the sample region. The magnetic field was measured with either an aluminum or fluorine nuclear-magnetic-resonance probe, depending on the strength of the field.

An attempt was made to field cool the dHvA samples so that data could be taken with \vec{H} parallel to \vec{q} , and \vec{H} perpendicular to \vec{q} and parallel to a $\langle 100 \rangle$ axis. After the crystals had been cooled through T_N in a large magnetic field along a $\langle 100 \rangle$ direction (the " \vec{q} " direction), ten or more field sweeps were made for \vec{H} parallel to \vec{q} and \vec{H} perpendicular to \vec{q} . The dHvA oscillations were digitally recorded on punched paper tape and later computer analyzed using a fast-Fourier algorithm described by Cooley and Tukey.²¹ Frequencies which consistently appeared in the dHvA spectrum were averaged together with an rms deviation of 0.5%. If the averaged frequencies for \vec{H} parallel to \vec{q} and \vec{H} perpendicular to \vec{q} were different, then the crystal was considered to be field cooled. On this basis the pure-Cr, 0.09-at.% V, and 0.58-at.% V samples appeared to be field cooled.

Recent optical data of Bos and Lynch²² indicated that a crystal with 0.94-at.% Mn had a \vec{q} which was commensurate with a reciprocal-lattice vector. The relative simplicity of the dHvA spectrum observed in the 0.91-at.% Mn sample indicated that this crystal was probably in the commensurate state. In this sample the dHvA data were taken as a function of crystal direction in a magnetic field of 40–57 kG, which corresponds to approximately 150–200 oscillations in the data for signals in the $(18-23) \times 10^6$ -G range.

III. RESULTS AND DISCUSSION

The discussion of the data will be divided into two sections. Section III A will discuss the data obtained from alloys in the incommensurate state while Sec. III B will discuss the data obtained from an alloy sample believed to be in the commensurate state.

A. Incommensurate State

Many frequencies were observed in each of the samples for the two crystal directions along which data were taken. Inspection of the data showed that the changes in two frequencies could easily be fol-

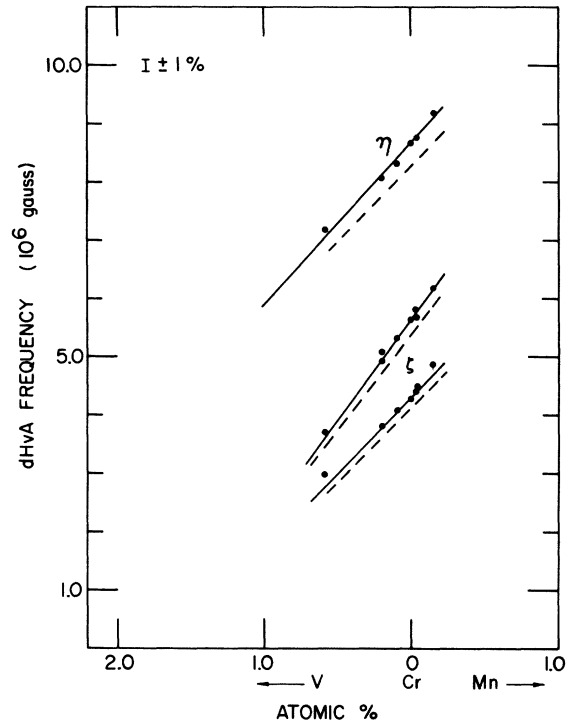


FIG. 3. dHvA frequencies measured along $[100]$ as a function of alloy concentration. The three frequencies arise from different truncations of the hole ellipsoids by the magnetic superlattice (see Ref. 15).

lowed, and that they correspond to the two branches labeled ζ by Graebner and Marcus.¹⁵ It was also possible to identify frequency η in the pure-Cr, 0.09-at.% V, and 0.58-at.% V samples. The change in dHvA frequencies ζ and η as a function of alloy concentration is shown in Fig. 3. It was assumed that frequencies lying close to the solid lines for the samples which were not field cooled also represent the frequency changes in ζ and η . In the case of ζ , this assumption is probably correct since for $\vec{H} \parallel \vec{q}$ there are no frequencies in this region. For η this assumption may be questionable since there are frequencies in this region for $\vec{H} \parallel \vec{q}$. dHvA frequencies were also observed in the 1.0-at.% V and 2.0-at.% V samples, but it was not possible to correlate these frequencies with those in pure Cr since the two samples were not field cooled.

The dashed lines in Fig. 3 show the calculated frequencies as a function of alloying, assuming that the size of the hole ellipsoids *does not* change with alloying but that only \vec{q} changes. That is, we assume that the orbit trajectories change with alloying only because of changes in the periodicity of the antiferromagnetic spin-density wave. This magnetic periodicity introduces new Bragg-reflection planes ("super-zone-boundaries") which qualitatively change the electronic orbits.²³ For the

calculation the dimensions of the hole ellipsoids determined by Graebner and Marcus (0.173, 0.234, and 0.268 \AA^{-1} for the semiaxes along the directions NH , $N\Gamma$, and NP , respectively)¹⁵ and the change in \vec{q} with alloying measured by Komura *et al.*⁸ were used. Since the calculated frequency for pure Cr differed slightly from the measured value, the calculated frequencies for pure Cr were normalized to the experimental values. The solid lines in Fig. 3 are the calculated dHvA frequencies for the alloys normalized to the experimental frequency measured for pure Cr.

The result of the normalization procedure was to use the conversion factors 109.3, 110.6, and 109.7 instead of the proper value 104.8 to convert areas in \AA^{-2} to frequencies in 10^6 G . The discrepancy between the calculated and measured frequencies probably arises since the truncated FS pieces used in the calculations have sharp edges, while those of the real FS pieces are probably slightly rounded.

The data for ζ and η are seen to be in agreement with the assumption that the size of hole ellipsoids does not change with alloying. The change in ζ and η can be explained by a change in the truncated FS piece due to a change in \vec{q} .

The rigid-band theorem assumes that the form of the density-of-states curve [$N(E)$ as a function of E] in an alloy system does not change with alloying and that $N(E_F)$ changes due to a change in the electron-to-atom ratio.²⁴ The magnetic properties, i. e., T_N and \vec{q} , of Cr-V-Mn ternary alloys are in agreement with the rigid-band theorem.⁸ A calculation using Heine's method²⁵ to determine the expected change in the dHvA period with alloying is of the wrong sign and is approximately four times smaller than the observed change in the lower ζ frequency. Since the ζ frequencies are associated with a hole piece, it might be expected that ζ increases with the addition of V. In contrast, our data show that the ζ frequencies decrease.

The assumption that the geometrical size of the hole ellipsoids does not change with alloying is consistent with the data. In the tight-binding approximation which has been used in analyzing specific-heat data on the transition-metal alloys,²⁶ the major contribution to the density of states in these alloys comes from the d bands, and the s bands give a constant contribution. In the Cr alloys this is consistent with the observed magnetic properties which depend on d -like parts of the FS and is also consistent with our data, since in this approximation the s -like FS pieces would remain relatively unchanged.

A second explanation for the consistency of the assumption with the data based on the band structure of Cr is that alloying changes the Fermi energy relative to the bands but the size of the hole ellipsoids does not change significantly. For example, using the band calculations of Asano and Yama-

shita,²⁷ one can estimate that 0.5-at.% V impurity changes the size of the hole ellipsoids less than 3%. Since in the incommensurate state one measures only truncated pieces of the hole ellipsoids and not the entire ellipsoid, the experiment is not very sensitive to a 3% change in the total size of the hole ellipsoids.

B. Commensurate State

Although the data in Fig. 1 are not complete enough, the recent optical data of Bos and Lynch reveal that the alloy Cr-0.94-at.% Mn exhibits antiferromagnetism which is commensurate with the chemical lattice at low temperatures. In the commensurate state the number of energy gaps should be smaller than the number of energy gaps in the incommensurate state. Because commensurate antiferromagnetism exhibits periodicity twice that of the chemical lattice, the occurrence of energy gaps can be investigated by calculating the energy bands for Cr in a simple-cubic Brillouin zone. Asano and Yamashita²⁷ have shown that the energy bands for the commensurate state can be obtained by remapping the paramagnetic energy bands calculated for a bcc zone into a simple-cubic zone. Energy gaps occur where bands of the same character intersect. They find an energy gap that is associated with the disappearance of large portions of the body of the electron jack and the hole octahedron. Their calculations also show that energy gaps occur in the hole ellipsoids at N and at the balls of the electron jack, at the points where these pieces are connected by \vec{q} , the spin-density wave vector.

The data for the 0.91-at.% Mn crystal are shown in Figs. 4 and 5 for the (010) and (110) planes, respectively. The data in Fig. 4 represent the average of dHvA signals from three separate runs, and hence there is less scatter in the data points than in Fig. 5, which is from just one run. The peaks in the dHvA spectrum had intensities of 100–300 relative units in the frequency range $(10-13) \times 10^6 \text{ G}$, 500–5000 relative units in the $(18-20) \times 10^6 \text{ G}$ range, and 50–100 relative units for frequencies near $22.8 \times 10^6 \text{ G}$. The increasing frequency branches starting at $10.2 \times 10^6 \text{ G}$ at [001] could be followed easily for $\pm 50^\circ$ in any direction from [001]. The decreasing frequency branch starting at $17 \times 10^6 \text{ G}$ at [001] had small amplitudes (~ 50 relative units) and could not be as easily followed, as indicated by the scatter in the data. It is possible that these are not real frequencies, considering their weak amplitudes compared to the amplitudes of the signals near 10.2 and $(18-20) \times 10^6 \text{ G}$. In the $(1\bar{1}0)$ plane the lower branch is not continuous through [110] and the relative amplitudes of the decreasing higher branch are the same as in the (010) plane. The solid lines represent the angular frequency variation of the function $A_0/(1-B \tan^2 \theta)$, which qualitatively fits the

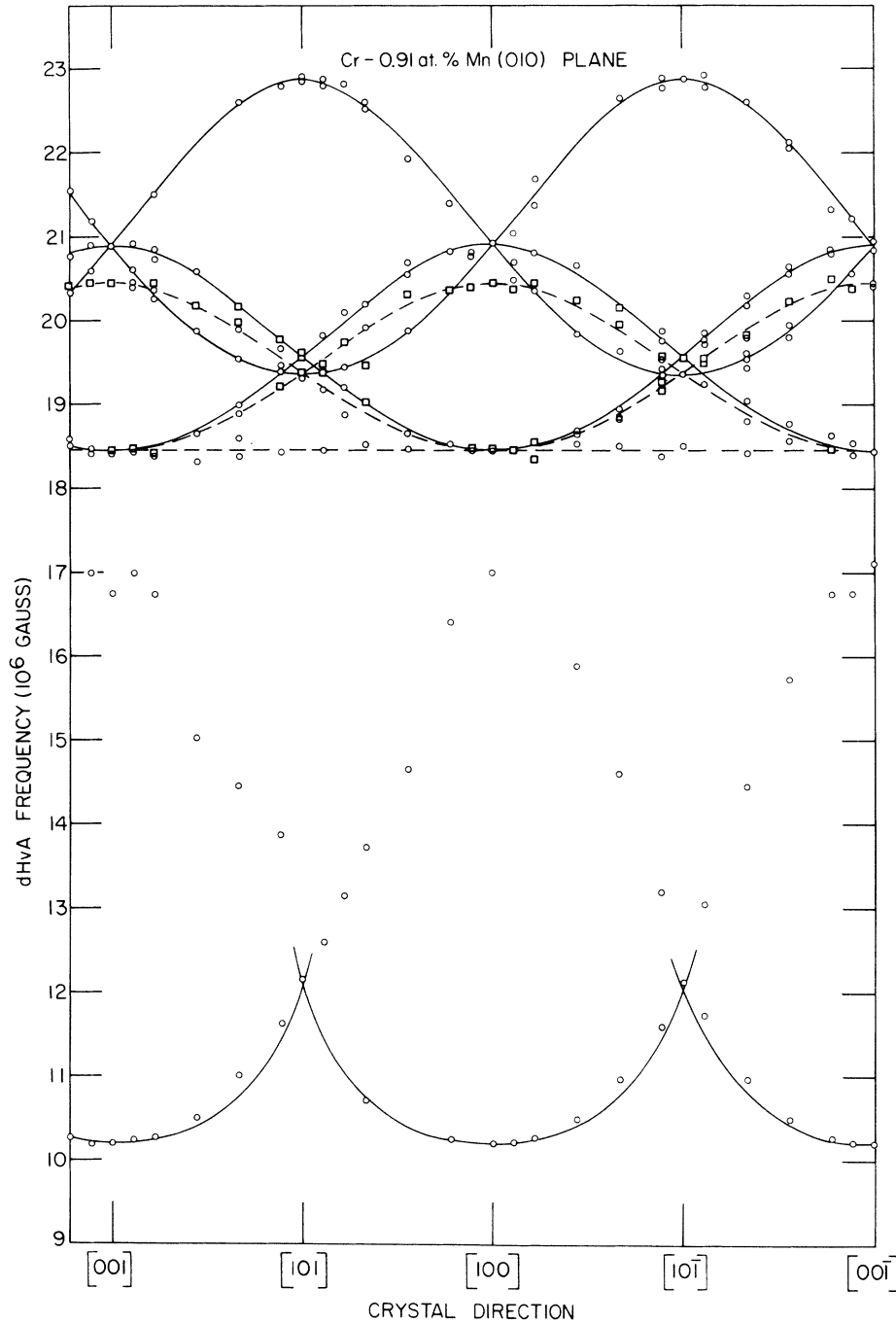


FIG. 4. dHvA data as a function of crystal direction in the Cr-0.91-at. % Mn sample for the (010) plane.

data. No special significance is attached to this.

In the high-frequency region $[(18-23) \times 10^6 \text{ G}]$ there were several distinct frequency branches. The strongest signals are represented by boxed points. The less intense signals in this region were usually stronger than the strongest signals in the low-frequency region $[(10-17) \times 10^6 \text{ G}]$. Each of the field sweeps contained 150-200 dHvA oscillations with a resolution of approximately 0.5%. Assuming an

ellipsoid of revolution model and using the frequencies $(18.5 \text{ and } 20.4) \times 10^6$ at $[001]$, the angular frequency variations were calculated for three pairs of ellipsoids of revolution on the $\langle 100 \rangle$ axes. The calculated results are indicated by dashed lines in Figs. 4 and 5. These lines account for the strongest signals and also for the angular-independent frequency of $18.5 \times 10^6 \text{ G}$ (associated with a circular cross-sectional area).

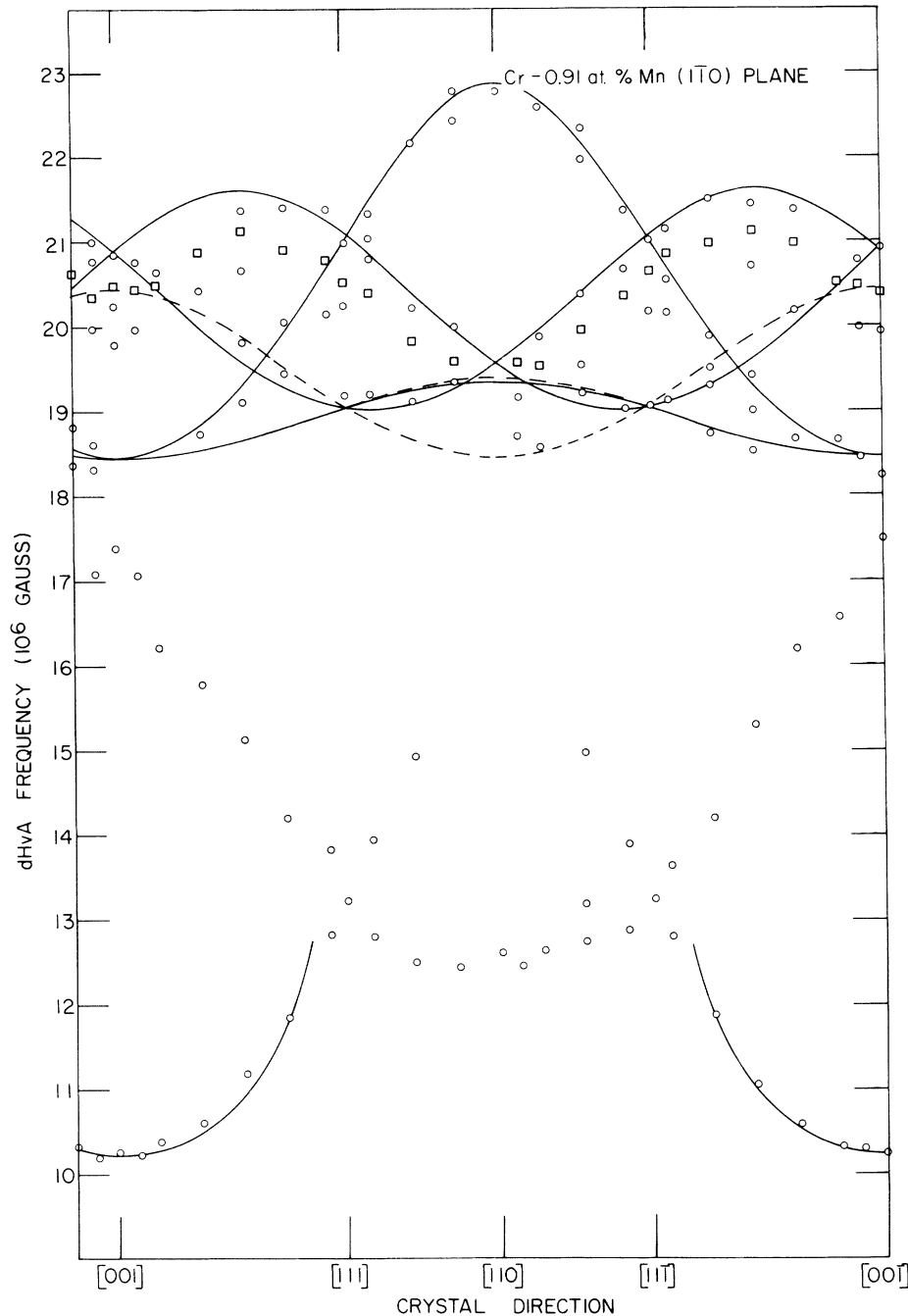


FIG. 5. dHvA data as a function of crystal direction in the Cr-0.91-at. % Mn sample for the (110) plane.

The less intense frequencies in the high-frequency region exhibited an angular dependence similar to the ρ frequencies associated with the hole ellipsoids in tungsten.²⁸ The lowest frequency (18.5×10^6 G) at [001] and the lowest and highest frequencies [(19.4 and 22.9×10^6 G) at [101] were assumed for the three principal cross-sectional areas of an ellipsoid. The angular frequency variations for six pairs of ellipsoids at N in the bcc Brillouin zone were calculated and are shown by solid lines in

Figs. 4 and 5. Notice that the data points in the (110) plane (Fig. 5) are not in as good agreement with the calculated curves as those in the (100) plane (Fig. 4). The agreement between the data points and the solid lines is considered reasonable.

In the (110) plane, the strongest signals have a maximum deviation of about 2% in the $\langle 111 \rangle$ directions from the curves calculated for a regular ellipsoid. One gets reasonable agreement between the angular variation of the data and the two curves

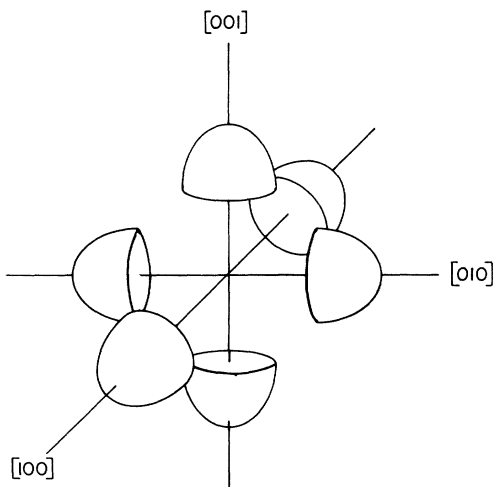


FIG. 6. Possible shape and orientation of the six remnants of the hole octahedra after the magnetic interaction occurs.

which intersect at 20.9×10^6 G at $[001]$ if the curves are shifted down to 20.4×10^6 G. Perhaps this is an indication that the ellipsoids are distorted.

We suggest that the regular ellipsoids are associated with the hole ellipsoids at $N(M)$, the ellipsoids of revolution with the same electron pieces at X , and the low-frequency signals with the remaining pieces of the hole octahedron after the antiferromagnetic interaction. The latter are conjectured to be remnants of the tips of the hole octahedra which are adjacent to the electron jack along ΓH .

Several arguments can be made for the identification of the low-frequency branches with the remnants of the hole octahedron. First, the angular dependence of the increasing branch (starting at 10.2×10^6 G) is the same in both the (010) and $(\bar{1}\bar{1}0)$ planes to within the experimental accuracy, suggesting circular symmetry about a $\langle 100 \rangle$ axis. The small amplitude of the signals suggests a large effective mass which could be due to holes in the d bands which have small mobilities and/or a large radius of curvature of the FS, both of which could be true for the remnant pieces. Finally, if the remnants are imagined to have the shape and orientation shown in Fig. 6, one can understand the absence of a third branch in the low-frequency region. The remnant along $[010]$ always has an orbit around the flat face and hence a large effective mass. This branch would be very difficult to observe.

Graebner²⁹ has suggested that the low-frequency branch is due to a truncation of the hole ellipsoids by the spin-density wave which results in two pieces of the FS. In his model the larger of these pieces gives rise to dHvA signals in the high-frequency re-

gion $[(18-23) \times 10^6$ G], while the smaller piece gives rise to signals in the $(10-17) \times 10^6$ -G region. However, unless fortuitous degeneracies occur in the FS, there should be three branches of the low-field data $[(10-17) \times 10^6$ G] in the (010) plane, while only two branches are observed; also, the angular data should be continuous, whereas the observed data are discontinuous in the vicinity of $[110]$ in the $(\bar{1}\bar{1}0)$ plane. It is interesting to notice that our Cr-0.91-at.% Mn data agree well with Graebner's data from a Cr-1.7-at.% Mn sample. We note that both samples exhibit commensurate antiferromagnetism, but beyond this offer no explanation for this agreement. To within experimental error, the data appear to be consistent with both Graebner's and our interpretation.

The FS dimensions calculated using the ellipsoid models are 0.218 , 0.257 , and 0.270 \AA^{-1} along the lines MH , $M\Gamma$, and MR , respectively, for the regular ellipsoids and 0.225 , 0.249 , and 0.249 \AA^{-1} for the $X\Gamma$ direction and directions perpendicular to $X\Gamma$, respectively. The regular ellipsoids are tentatively identified with the hole ellipsoids, while the ellipsoids of revolution are thought to be associated with small electron pieces at X . These dimensions, along with the results of Asano and Yamashita's calculations,²⁷ are shown in Fig. 7.

IV. CONCLUSIONS

The dHvA data for incommensurate and commen-

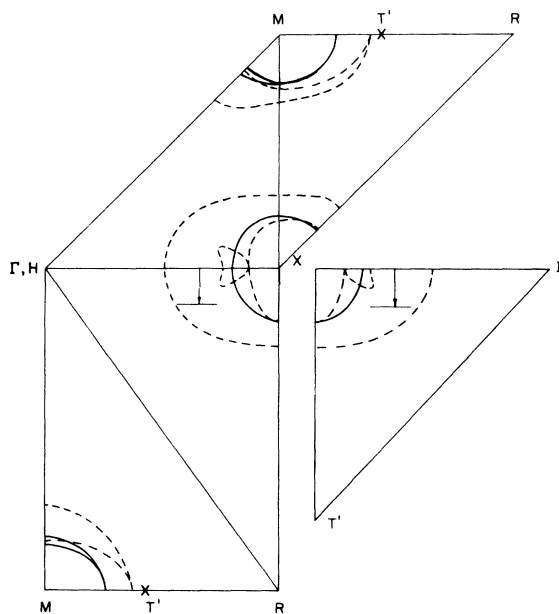


FIG. 7. FS pieces determined from the data on the Cr-0.91-at.% Mn sample are shown by solid lines. The FS calculations of Asano and Yamashita are shown by the dashed lines.

surate antiferromagnetic Cr-rich alloys are further evidence for the existence of hole ellipsoids in Cr. The data from the incommensurate alloys can be interpreted on the assumption that the size of the hole ellipsoids does not change for small impurity concentrations. The dHvA frequency changes are then consistent with changes in \tilde{q} due to alloying.

In the case of the commensurate alloy, the present data are in reasonable agreement with the calculated frequency variations of a regular ellipsoid (hole ellipsoids) and an ellipsoid of revolution (electron pieces). Also, the data are consistent with

the existence of remnants of the hole octahedron.

ACKNOWLEDGMENTS

It is a pleasure to acknowledge the technical expertise of F. A. Schmidt, who produced the ingots from which we obtained our crystals. We also want to thank Dr. R. A. Phillips, Professor S. H. Liu, Professor S. K. Sinha, and Dr. R. P. Gupta for helpful discussions. One of us (E. J. G.) wishes to thank the National Aeronautics and Space Administration for support in the form of a NASA Traineeship.

*Work performed in the Ames Laboratory of the U. S. Atomic Energy Commission. Contribution No. 3030. Work based on Ph.D. thesis submitted by E. J. Gutman to the Graduate College, Iowa State University.

[†]Present address: Department of Physics, University of Illinois, Urbana, Ill. 61801.

¹W. C. Koehler, R. M. Moon, A. L. Trego, and A.R. Mackintosh, Phys. Rev. 151, 405 (1966).

²A. L. Trego and A. R. Mackintosh, Phys. Rev. 166, 495 (1968).

³G. De Vries, J. Phys. Radium 20, 438 (1959).

⁴M. A. Taylor, J. Less-Common Metals 4, 476 (1962).

⁵Y. Hamaguchi and N. Kunitomi, J. Phys. Soc. Japan 19, 1849 (1964).

⁶Y. Hamaguchi, E. O. Wollan, and W. C. Koehler, Phys. Rev. 138, A737 (1965).

⁷F. Heininger, Physik Kondensierten Materie 5, 285 (1966).

⁸S. Komura, Y. Hamaguchi, and N. Kunitomi, J. Phys. Soc. Japan 23, 171 (1967).

⁹H. Ohno, T. Suzuki, and H. Takaki, J. Phys. Soc. Japan 23, 251 (1967).

¹⁰S. Arajs, J. Appl. Phys. 39, 673 (1968).

¹¹S. Arajs, Can. J. Phys. 47, 1005 (1969).

¹²W. M. Lomer, Proc. Phys. Soc. (London) 80, 489 (1962).

¹³W. M. Lomer, Proc. Phys. Soc. (London) 84, 327 (1964).

¹⁴T. L. Loucks, Phys. Rev. 139, A1181 (1965).

¹⁵J. E. Graebner and J. A. Marcus, Phys. Rev. 175,

659 (1968).

¹⁶R. A. Montalvo and J. A. Marcus, Phys. Letters 8, 151 (1964).

¹⁷E. J. Gutman and J. L. Stanford, Bull. Am. Phys. Soc. 15, 264 (1970).

¹⁸R. W. Stark and L. R. Windmiller, Cryogenics 8, 272 (1968).

¹⁹D. R. Stone, Ph.D. thesis (Iowa State University of Science and Technology, 1967) (unpublished).

²⁰D. J. Boyle, Ph. D. thesis (Iowa State University of Science and Technology, 1968) (unpublished).

²¹J. W. Cooley and J. W. Tukey, Math. Comput. 19, 297 (1965).

²²L. W. Bos and D. W. Lynch, Phys. Rev. B 2, 4567 (1970).

²³L. M. Falicov and M. J. Zuckermann, Phys. Rev. 160, 372 (1967).

²⁴N. F. Mott, Advan. Phys. 13, 325 (1964).

²⁵V. Heine, Proc. Phys. Soc. (London) A69, 505 (1956).

²⁶C. H. Cheng, C. T. Wei, and P. A. Beck, Phys. Rev. 120, 426 (1960).

²⁷S. Asano and J. Yamashita, J. Phys. Soc. Japan 23, 714 (1967).

²⁸R. F. Girvan, A. V. Gold, and R. A. Phillips, J. Phys. Chem. Solids 29, 1485 (1968).

²⁹J. E. Graebner, in *Proceedings of the Twelfth International Conference on Low Temperature Physics, Kyoto, Japan*, edited by Eizo Kanda (Academic Press of Japan, Kyoto, Japan, 1971), p. 601.